臺灣醫用迴旋加速器學會暨中華民國核醫學學會
109年度學術推廣教育暨繼續教育學術研討會

放射藥物的發展與設計

Ling-Wei Hsin, Ph.D.（忻凌偉）

[1] Molecular Probes Development Core, Molecular Imaging Center,
[2] Center for Innovative Therapeutics Discovery, and
[3] School of Pharmacy, National Taiwan University

August 29, 2020

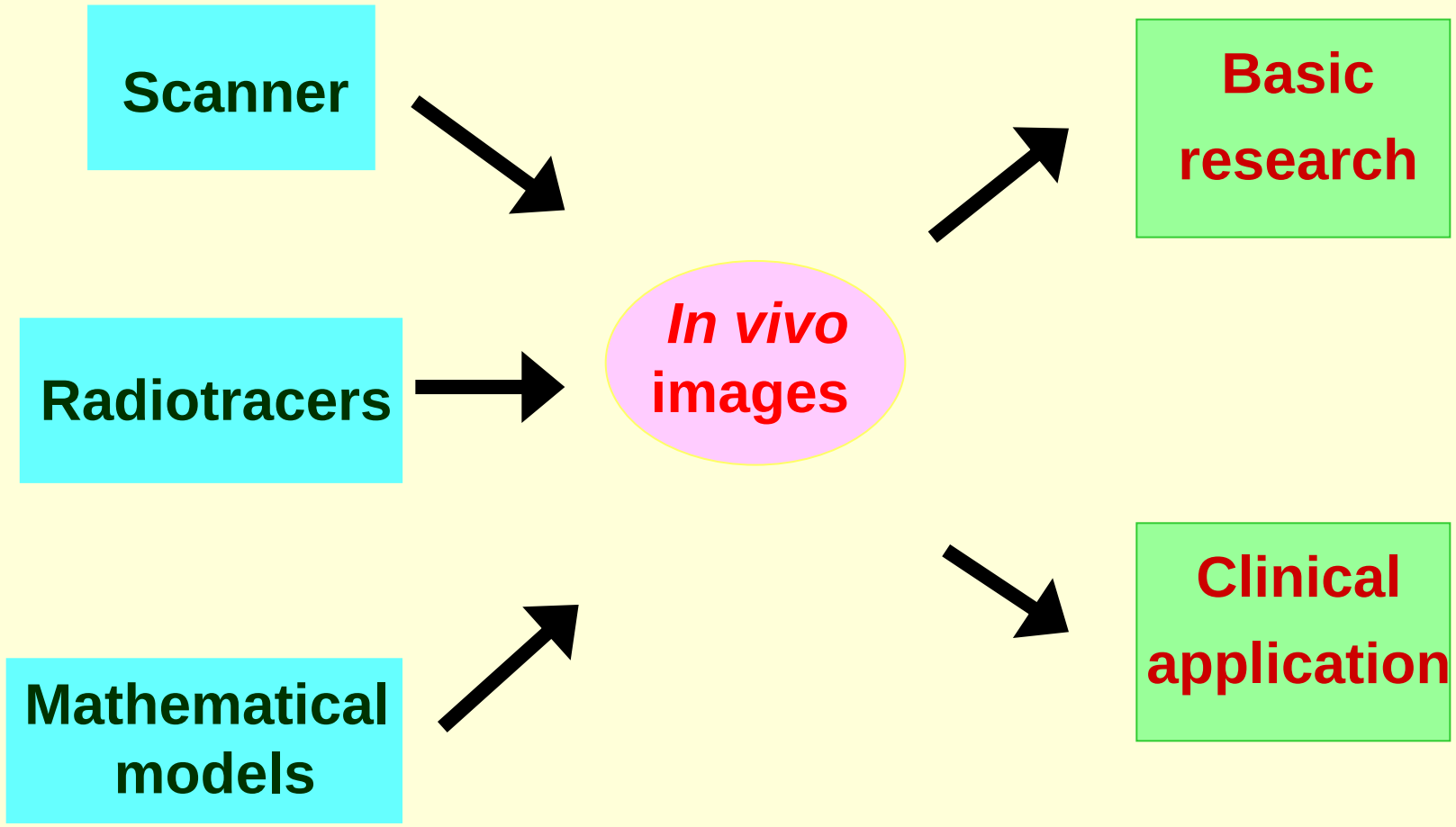
Scanner
Radiotracers
Mathematical models
In vivo images
Basic research
Clinical application

Medicinal Chemistry

Synthesis → ***Drug*** →

Dissolution

Absorption

Distribution

Accumulation

Metabolism

Excretion

Central Nervous System Acting Drugs

1. **Lipophilicity**
2. **Metabolic Stability**
3. **Distribution**
4. **Target-Selectivity**
5. **Central versus Peripheral-Selectivity**

Physicochemical Properties

- Acid/base properties
- Water solubility
- Partition coefficient
- ~~Crystal structure~~
- Stereochemistry

Acid/Base Properties

- Directly affect **distribution**, **metabolism**, and **excretion**.

Eq. 2.1

$$\underset{\text{Acid (acetic acid)}}{CH_3COOH} + \underset{\text{Base (water)}}{H_2O} \rightleftharpoons \underset{\text{Conjugate base (acetate)}}{CH_3COO^{\ominus}} + \underset{\text{Conjugate acid (hydronium)}}{H_3O^{\oplus}}$$

Eq. 2.2

$$\underset{\text{Base (methylamine)}}{CH_3NH_2} + \underset{\text{Acid (water)}}{H_2O} \rightleftharpoons \underset{\text{Conjugate Acid (methylammonium)}}{CH_3NH_3^{\oplus}} + \underset{\text{Conjugate base (hydroxide)}}{{}^{\ominus}OH}$$

Acidic Compounds

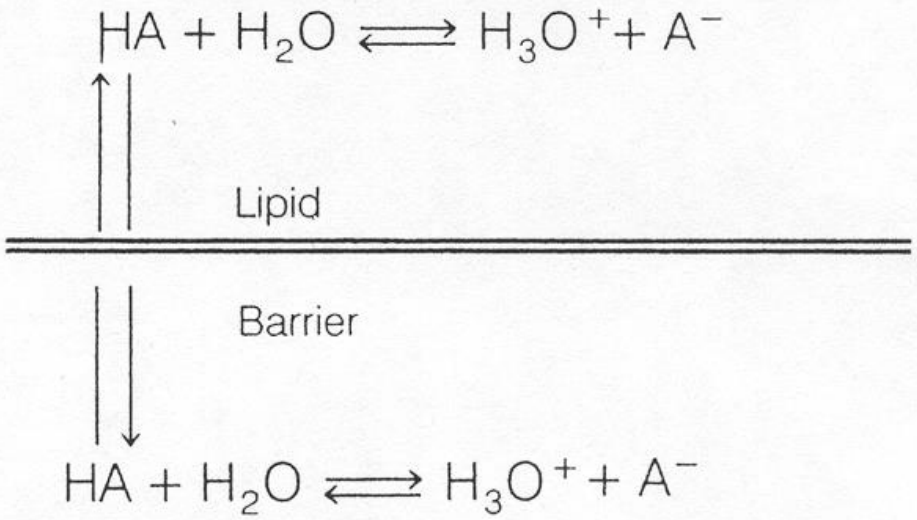

FIG. 2-3. *Passage of HA acids through lipid barriers.*

Basic Compounds

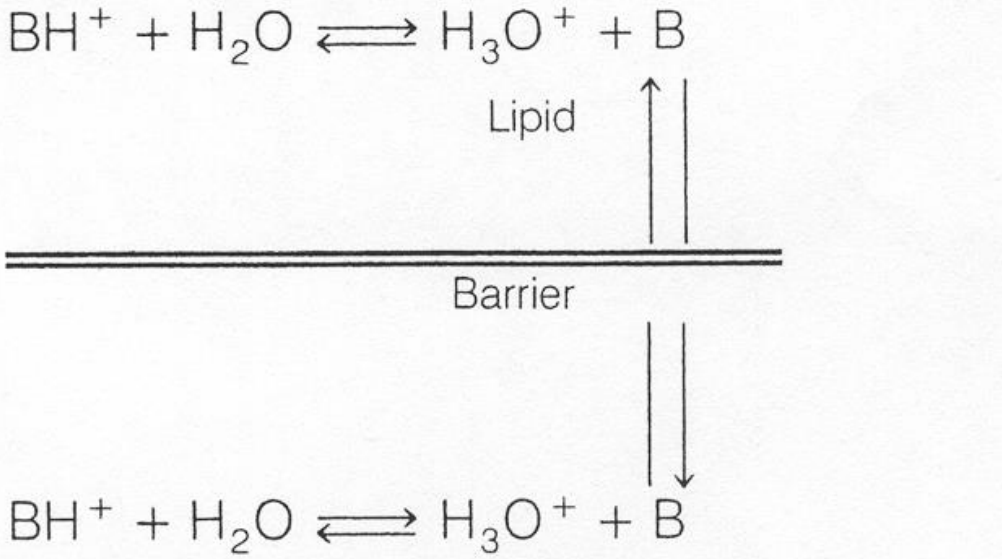

FIG. 2-4. *Passage of BH^+ acids through the lipid barrier.*

Acid/Base Properties

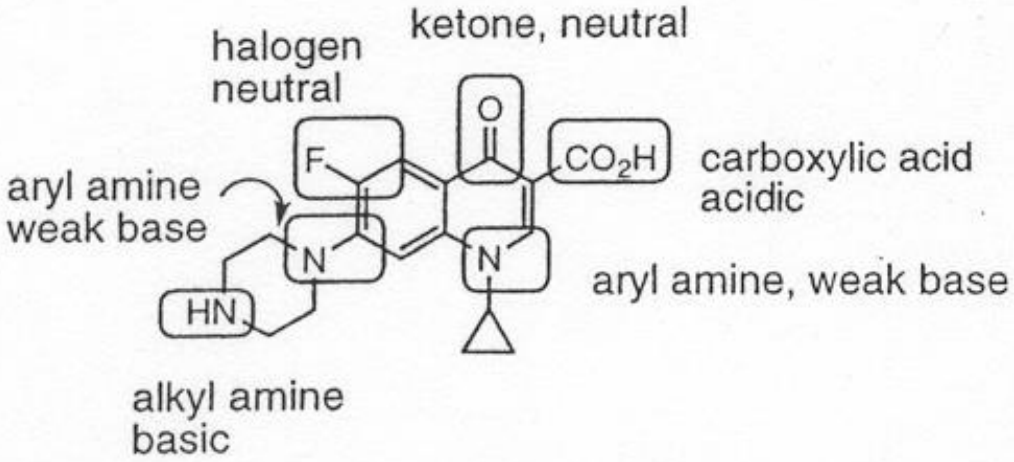

Fig. 2.4. Chemical structure of ciprofloxacin showing the various organic functional groups.

Acid/Base Properties

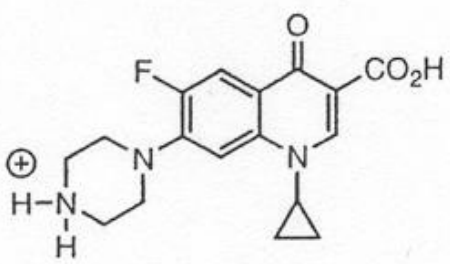

Stomach (pH 1.0 – 3.5)

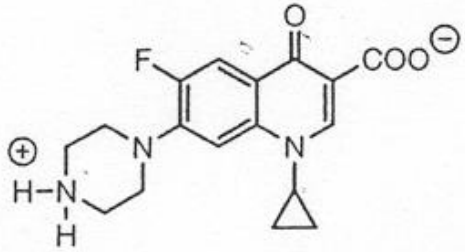

Duodenum (pH ~4)

Fig. 2.5. Predominate forms of ciprofloxacin at two different locations within the gastrointestinal tract.

Table A-2. pH Values for Tissue Fluids

Fluid	pH
Aqueous humor	7.2
Blood, arterial	7.4
Blood, venous	7.4
Blood, maternal umbilical	7.3
Cerebrospinal fluid	7.4
Duodenum	5.5
Feces[a]	7.12 (4.6–8.8)
Ileum, distal	8.0
Intestine, microsurface	5.3
Lacrimal fluid (tears)	7.4
Milk, breast	7.0
Muscle, skeletal[b]	6.0
Nasal secretions	6.0
Prostatic fluid	6.5
Saliva	6.4
Semen	7.2
Stomach	1.0–3.5
Sweat	5.4
Urine	5.8 (5.5–7.0)
Vaginal secretions, premenopause	4.5
Vaginal secretions, postmenopause	7.0

[a] Value for normal soft, formed stools; hard stools tend to be more alkaline, whereas watery, unformed stools are acidic.
[b] Studies conducted intracellularly on the rat.

Water Solubility

- The solubility of a drug molecule in water greatly affects the **routes of administration** available and its **absorption**, **distribution** and **elimination**.

- **Hydrogen bond** forming potential of the functional groups and the **ionization** of functional groups.

Water Solubility vs Counter Ion

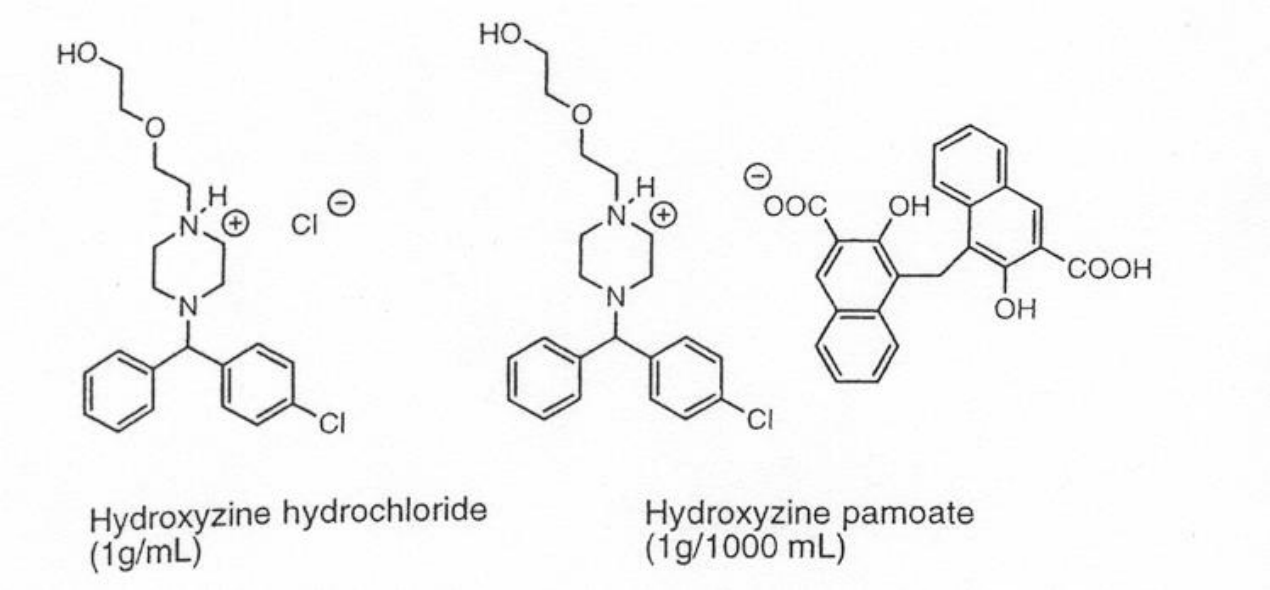

Hydroxyzine hydrochloride
(1g/mL)

Hydroxyzine pamoate
(1g/1000 mL)

Lipophilicity: logP

$$P = \frac{C_{organic}}{C_{aqueous}}$$

$$logP = \log \frac{C_{organic}}{C_{aqueous}}$$

Lipophilicity: logP

Table 2.6. Hydrophilic-lipophilic Values (π V) for Organic Fragments (9)

Fragments	π Value
C (aliphatic)	+0.5
Phenyl	+2.0
Cl	+0.5
O_2NO	+0.2
IMHB	+0.65
S	0.0
O = C−O (carboxyl)	−0.7
O = C−N (amide, imide)	−0.7
O (hydroxyl, phenol, ether)	−1.0
N (amine)	−1.0
O_2N (aliphatic)	−0.85
O_2N (aromatic)	−0.28

Eq. 2.7 $\quad \text{LogP} = \Sigma\pi \text{ (fragments)}$

Lipophilicity: logP

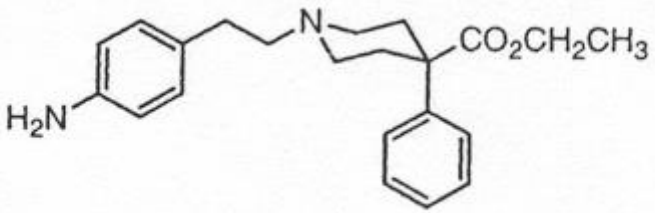

Fragments	π
2 amines	−2.0
9 aliphatic carbons	+4.5
2 phenyl rings	+4.0
1 ester	−0.7
logP	+5.8

Fig. 2.14. Calculation of logP for anileridine.

Stereochemistry and Drug Action

- Not only what functional groups are responsible for the drug's activity, but also what **three-dimensional orientation (3D)** of these groups is also needed.

Stereochemistry and Drug Action

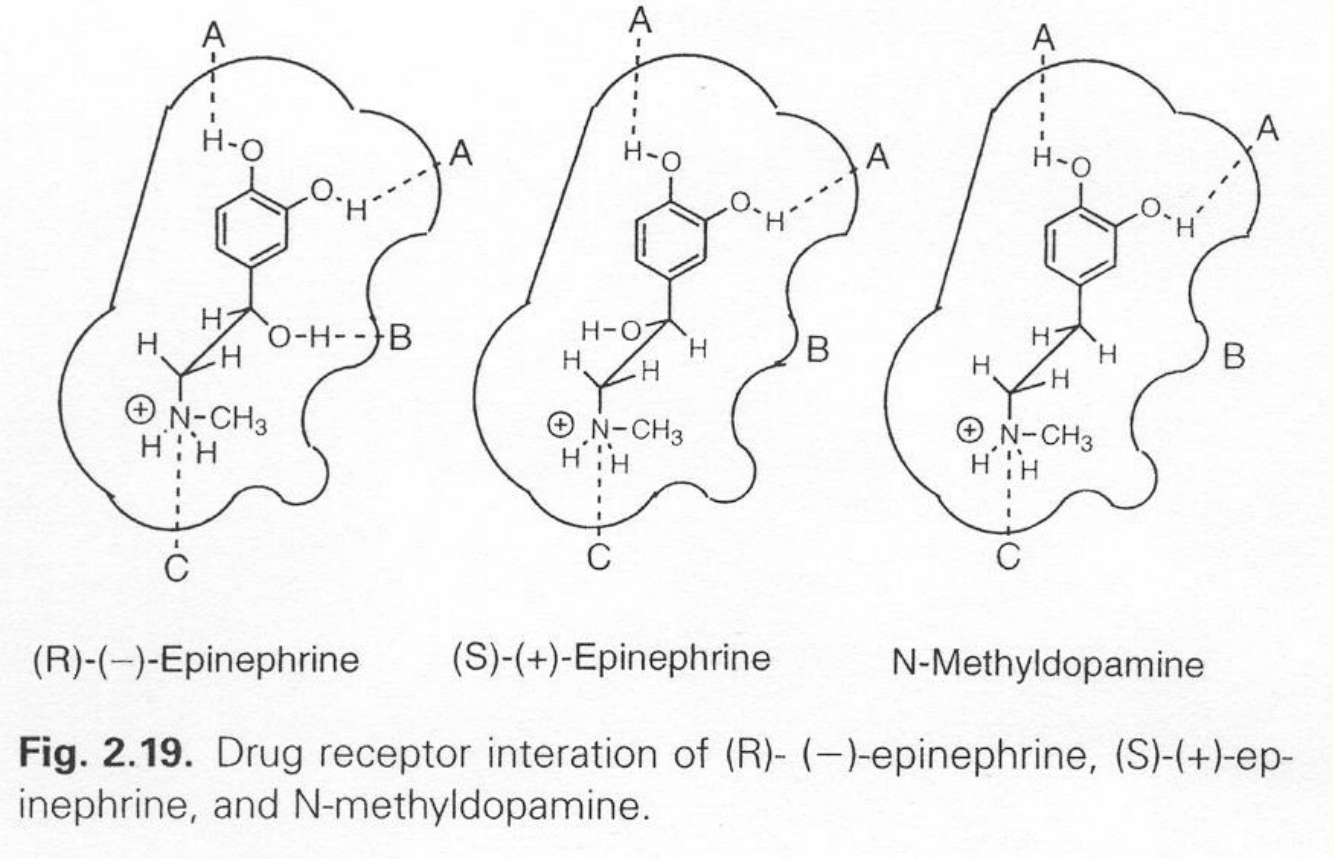

Fig. 2.19. Drug receptor interation of (R)- (−)-epinephrine, (S)-(+)-epinephrine, and N-methyldopamine.

Stereochemistry and Drug Action

- **Enantiomers** show significant differences in their **pharmacokinetic** and **pharmacodynamic** behavior. Such differences can result in **adverse side effects** or **toxicity** due to one of the isomers or the isomers may exhibit significant differences in **absorption** (especially active transport), **serum protein binding** and **metabolism**.

Ignoring Chirality?

Design of a PET Radiotracer

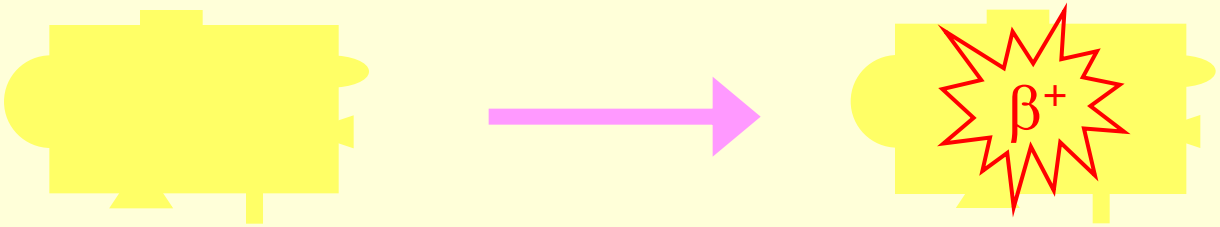

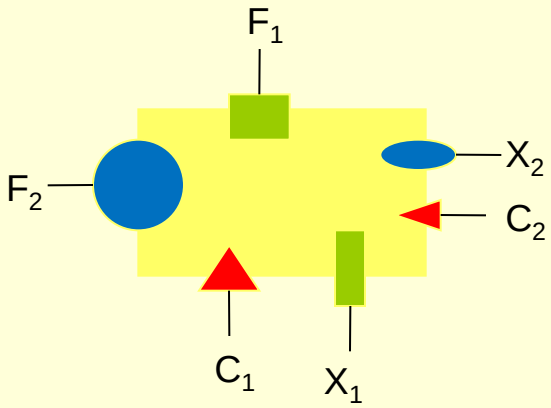

Selection of Radionuclide !

Design of a PET Radiotracer

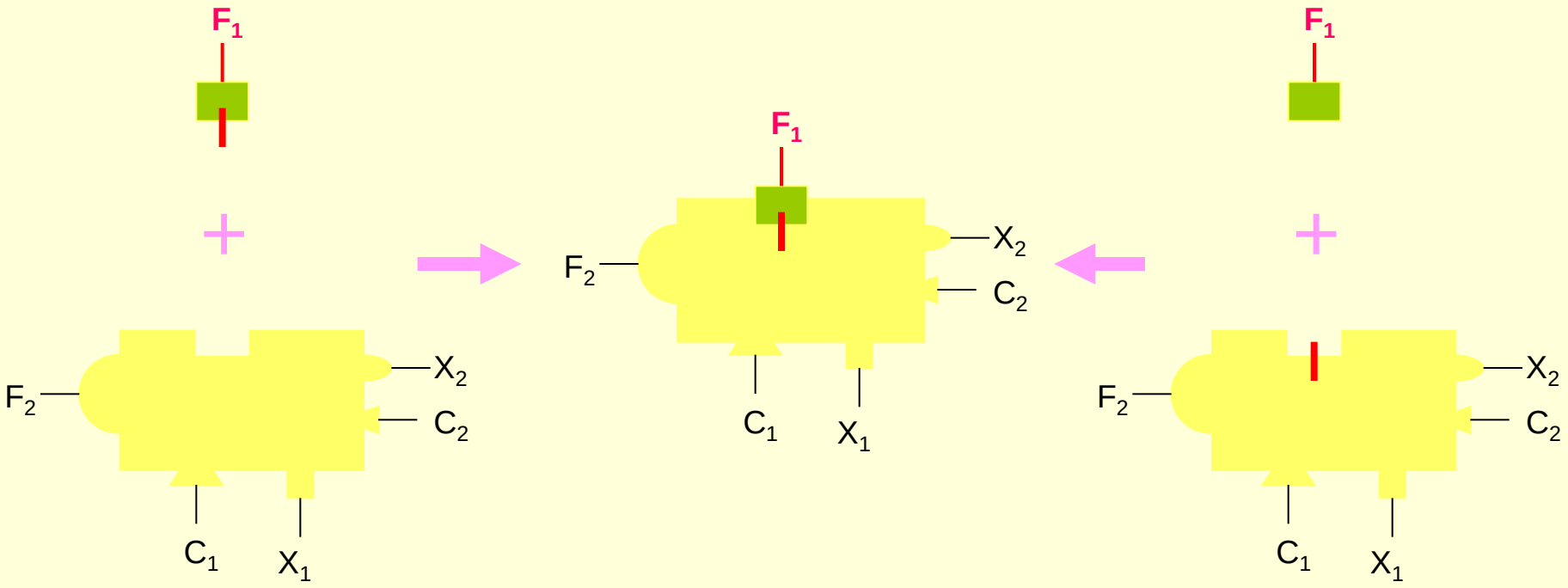

Nucleophilic ***Electrophilic***

Nucleophilic Substitution with Fluoride

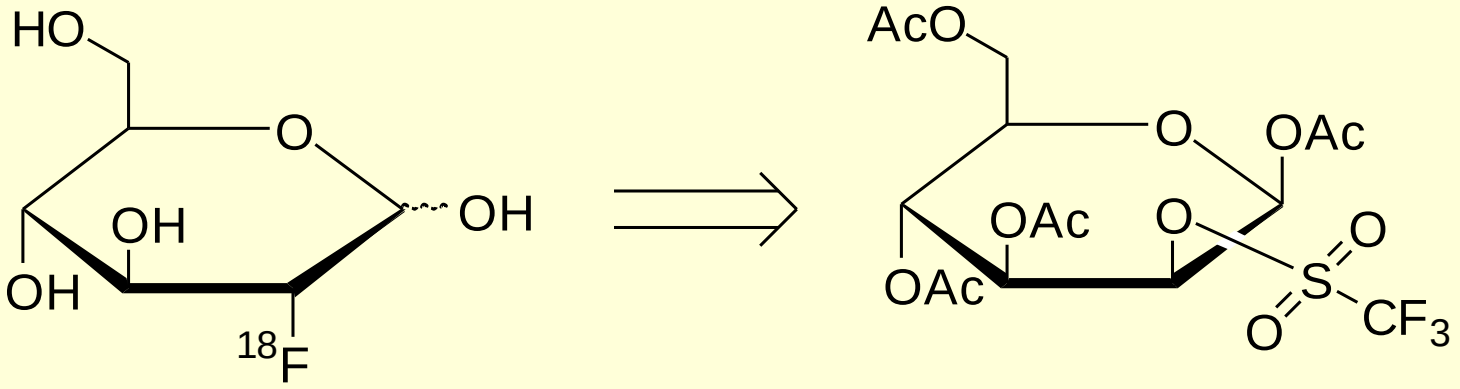

[^{18}F]FDG **Mannose Triflate**

Nucleophilic Substitution with Fluoride

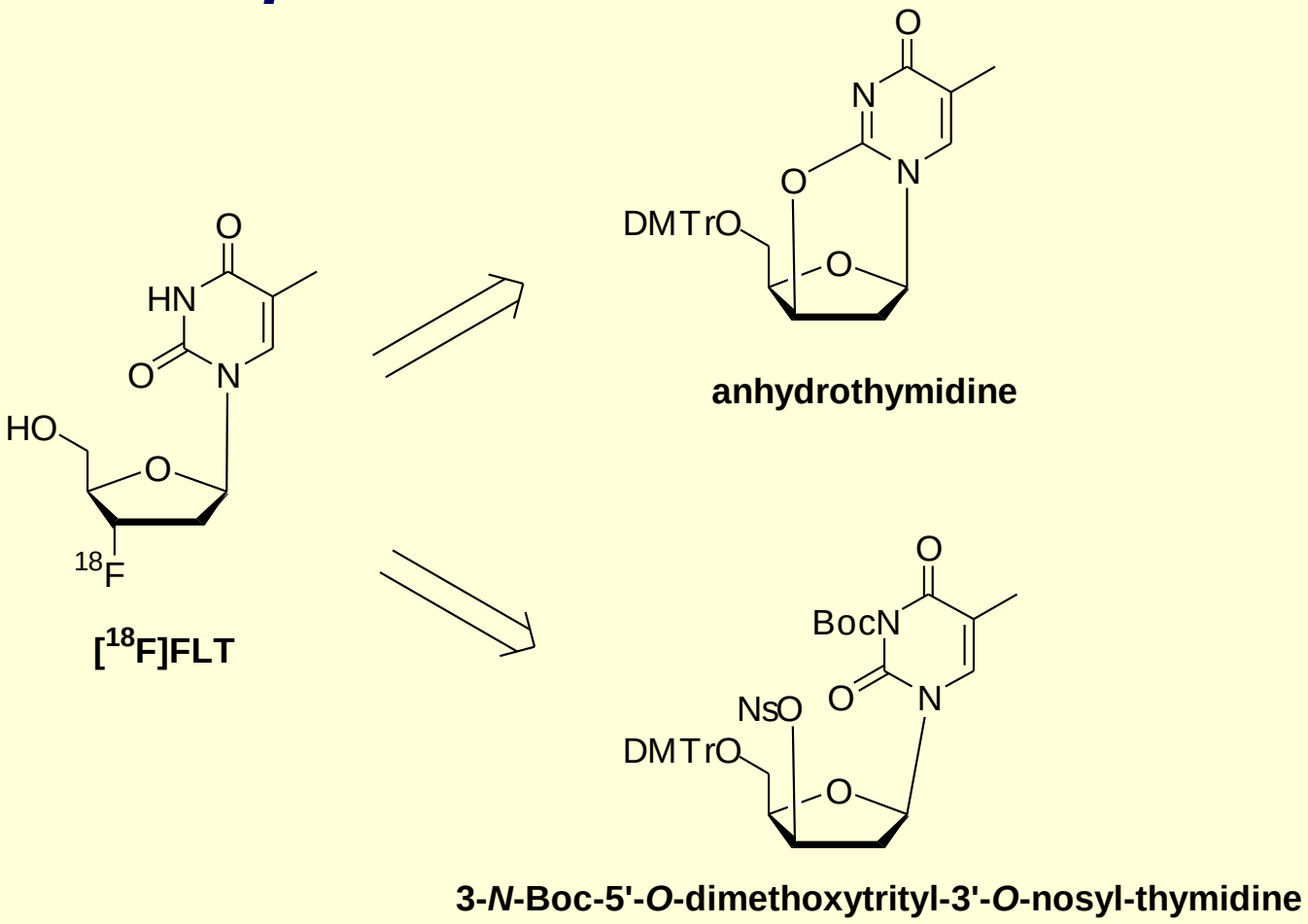

Nucleophilic Aromatic Substitution

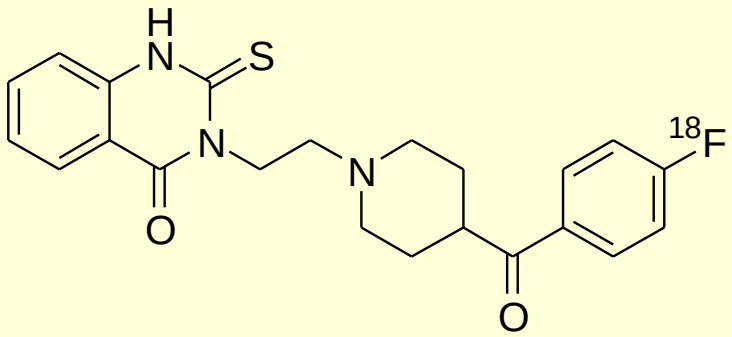

[^{18}F]fluoroaltanserin

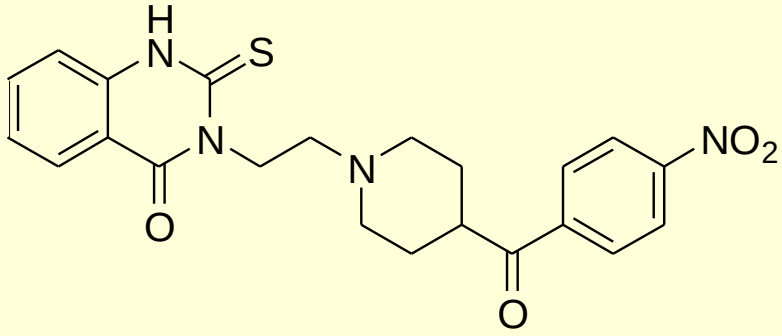

nitroaltanserin

Destannylfluorination

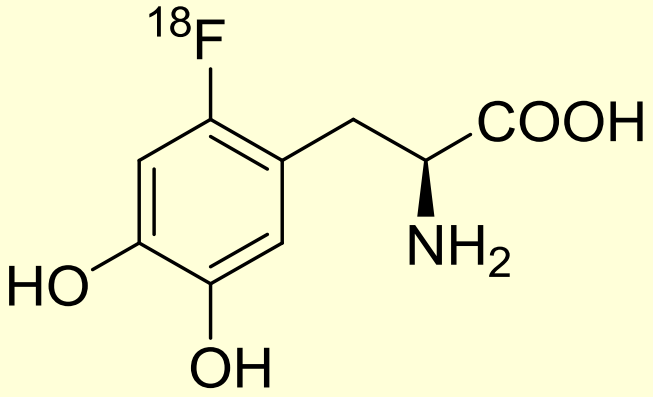

[^{18}F]Fluoro-*L*-DOPA

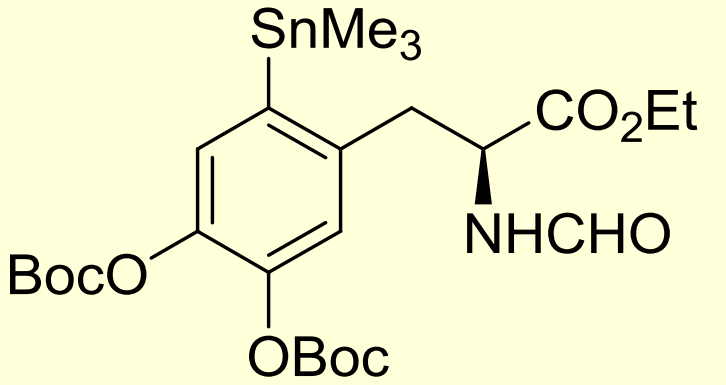

6-trimethylstannyl-*L*-Dopa

[^{18}F]-Fluoroethylcholine

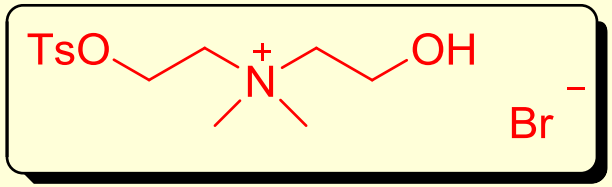

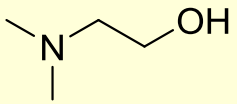

dimethylaminoethanol

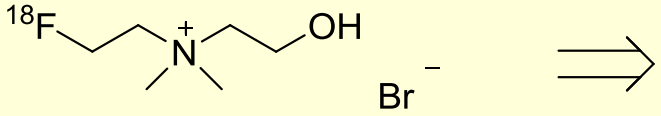

[^{18}F]fluoroethylcholine bromide

+

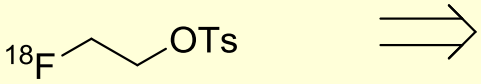

1,2-bis(tosyloxy)ethane

M_2 Receptor PET tracer

[^{18}F]-FP-TZTP

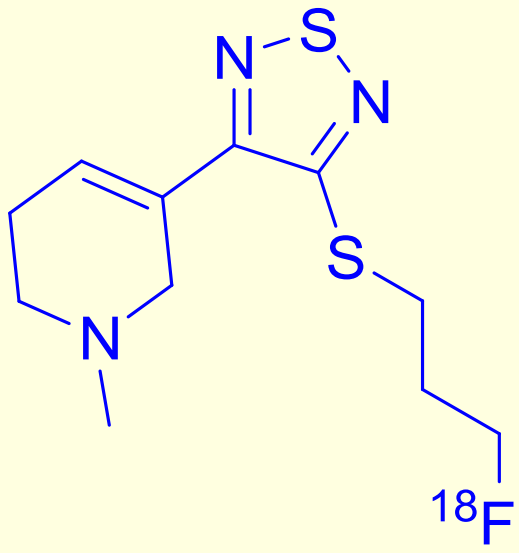

[^{18}F]-FP-TZTP

- **P-TZTP** showed a K_i of 23 nM for M1 and 1.5 nM for M2.
- **[^{18}F]-FP-TZTP** showed a K_i of 7.4 nM for M1 and 2.2 nM for M2; it did not bind to M3 receptors or other biogenic amine receptors.

[^{18}F]-FP-TZTP

- A major concern in PET studies is that the radioligand will metabolize to radioactive metabolites.
- To quantify receptors accurately, the time course of the parent compound in blood must be determined.
- Verify that radioactive metabolites do not cross the BBB.

[^{18}F]-FP-TZTP

- In rats, only 5% of plasma radioactivity was parent compound by 15 min post-injection.
- One metabolite was almost as lipophilic as the parent compoud as measured by TLC, suggesting that it might cross the BBB.
- Parent compound was found to represent greater than 95% of extracted radioactivity in rat brain through 30 min and greater than 90% at 45 and 60 min.

The Validation of FP-TZTP

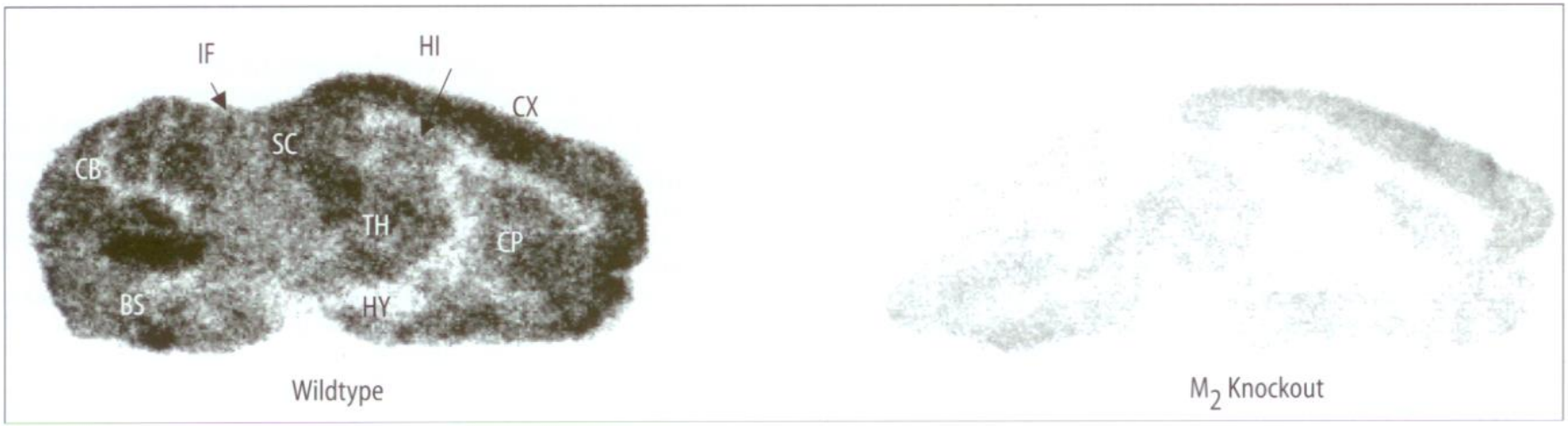

Figure 17.7. Regional brain localisation of [^{18}F]-FP-TZTP in M_2 knockout compared to wild-type mice at 30 minutes post-injection (sagittal slice ~1.8 mm from the midline). In the knockout mice, note the decrease in radioactivity an all grey matter regions with a high percentage of M2 receptors including cerebellum (CB), brain stem (BS) and thalamus (TH).

The Validation of FP-TZTP

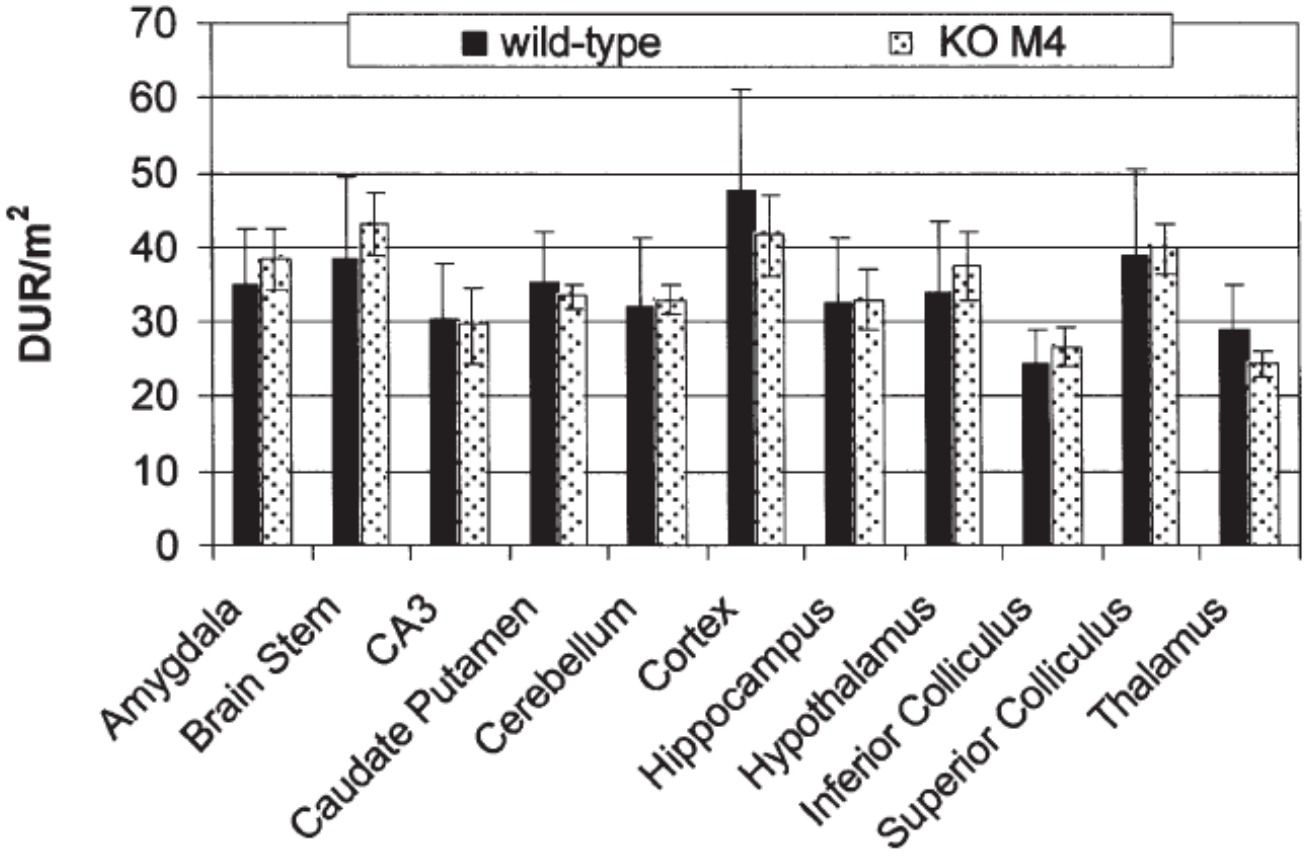

Fig. 7. Regional brain localization of [^{18}F]FP-TZTP in M4 KO compared to WT mice at 30 min after intravenous injection of ~300 μCi. (Data represent the mean DUR/m^2 ± S.D.; n = 5–7 mice).

Neuropharmacology 44 (2003) 653–661

The Validation of FP-TZTP

- Similar studies with M1 KO, M3 KO and M4 KO *vs* WT did **not** reveal a significant decrease in grey matter uptake.
- The metabolic profile of FP-TZTP was studied in rat and human hepatocytes using liquid chromatography and mass spectrometry and, compared with independently synthesized standards.

[^{18}F]-FP-TZTP Studies in Non-human Primates

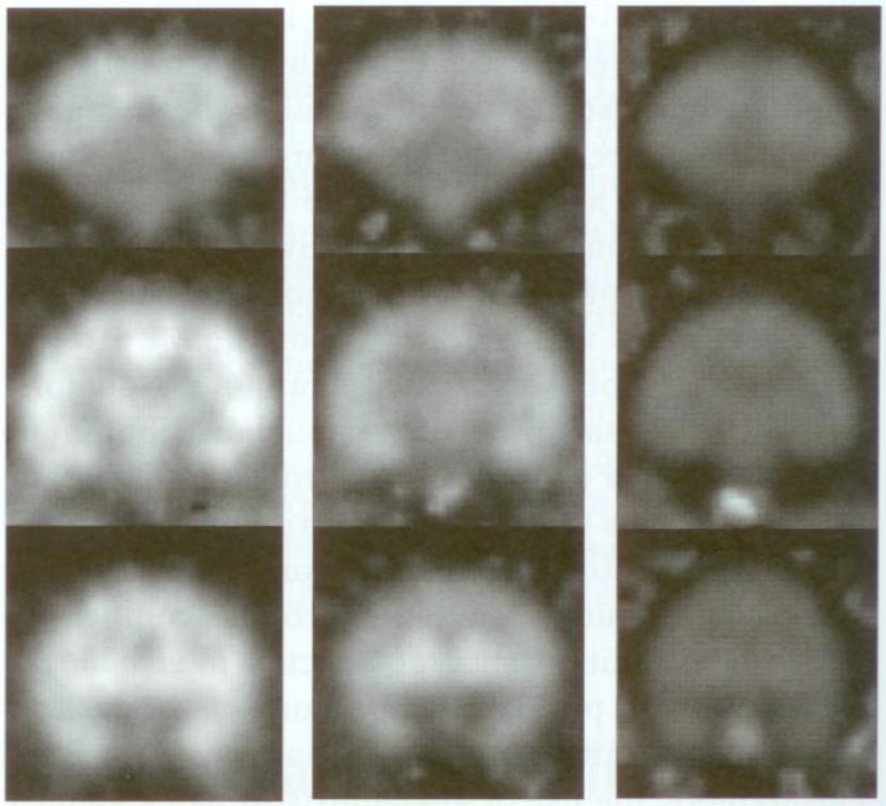

Figure 17.5. Distribution volume (*V*) images from [^{18}F]-FP-TZTP studies in monkey. Images are coronal slices and all data are scaled to maximum of 27ml/ml. (A) Control study with uniform cortical binding and lower cerebellar binding. (B) Physostigmine (200 mg/kg/hr) started 30 minutes before [^{18}F]-FP-TZTP with significant reduction in binding. C. Pre-blocking study with non-radioactive FP-TZTP (400 nM/kg) administered 5 minutes before [^{18}F]-FP-TZTP shows substantial reduction in binding.

- These experiments were used to develop the methodology and analysis techniques for human studies.

[^{18}F]-FP-TZTP Studies in Humans

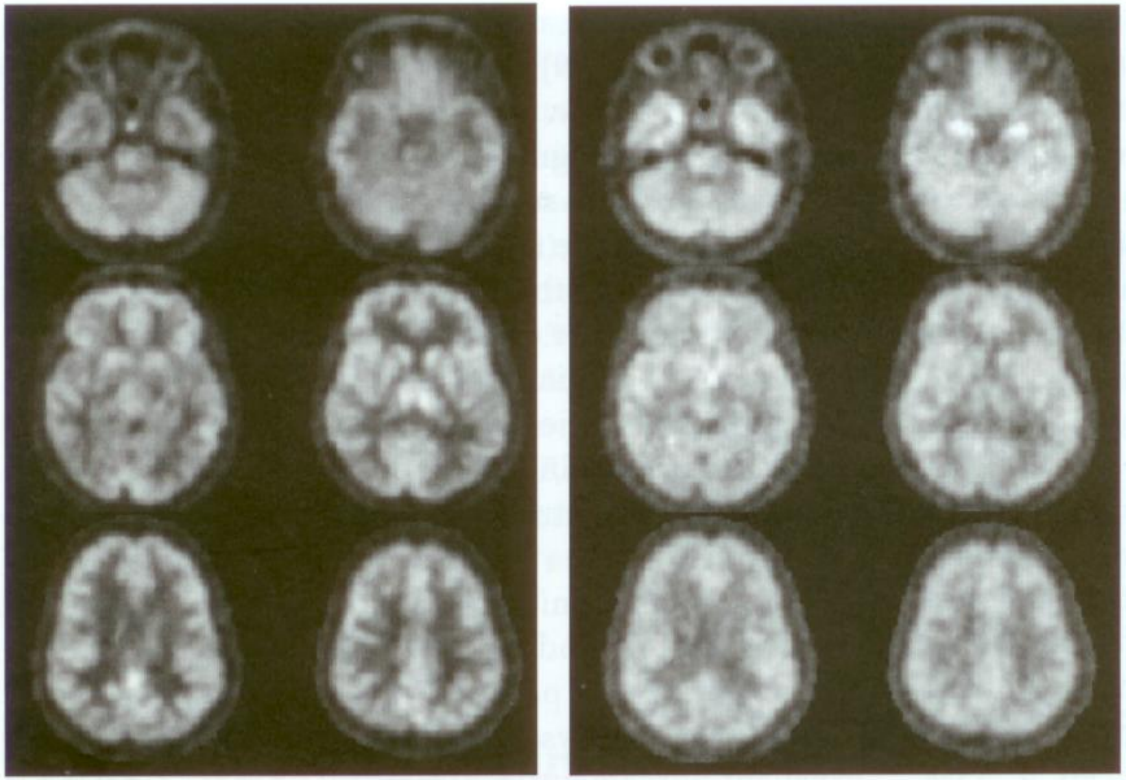

Figure 17.6. Sample K_1 and V images from [^{18}F]-FP-TZTP in a young control subject calculated by pixel-by-pixel fitting of the one tissue compartment model to 120 minutes of data. The K_1 and V images are displayed to a maximum of 0.7 ml/min/ml and 50 ml/ml, respectively. Note the relatively uniform cortical binding in the V image, except for the higher binding in the amygdala.

[^{18}F]-FP-TZTP Studies in Humans

- In the first clinical studies, an age-related increase in M2 receptor binding potential was observed.
- A reasonable hypothesis for the increased volume of distribution in elderly normal subiects with Apoe-E4 positive is a decreased concentration of ACh in the synapse.
- The use of **[18F]-FP-TZTP** can be considered an *in vivo* measurement of muscarinic systems biology, rather than the receptor density alone.

Novel Serotonin Transporter (SERT) Imaging Agents for PET

Bioorg. Chem., **2020**, 97, 103654.

Introduction

- Serotonin (5-HT) plays important roles in a wide variety of physiological functions through interaction with **14** serotonin receptor subtypes.
- In CNS, **serotonin transporters (SERT)** reuptake the released 5-HT from the synapse into the presynaptic nerves to terminate its downstream.
- Dysregulation of serotonin transmission is known to be involved in depression, anxiety, obsessive-compulsive disorder, eating disorder, addiction, Parkinson's disease, and Alzheimer's disease.

5-HT Synaptic Terminals

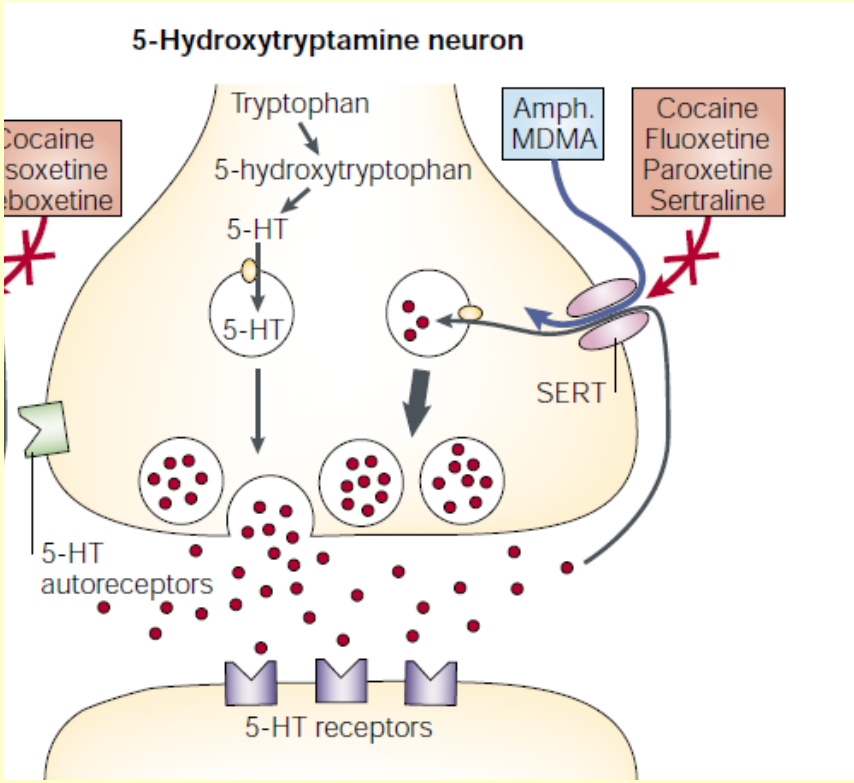

Torres, G. E. et al. *Nature Reviews Neuroscience* **2003**, *4*, 13.

Introduction

- SERT is the target of selective serotonin reuptake inhibitor **(SSRIs)**, which is among the most commonly prescribed class of antidepressants in last decades.
- There is a **lag time** before the onset of antidepressant effect of SSRIs and more than **30%** of patients are nonresponders.[7].
- By estimation of the **drug occupancy** of SERT binding sites by the antidepressant, **in vivo PET** or SPECT imaging studies could assist in the development of more effective approaches to the treatment of depression.

Bioorg. Chem., **2020**, 97, 103654.

SERT PET Tracers

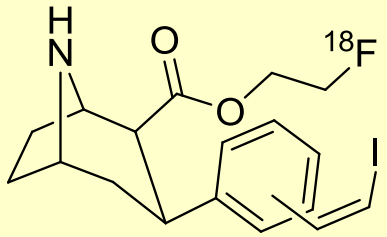

meta, **[^{18}F]FEt-*m*ZIENT**
para, **[^{18}F]FEt-*p*ZIENT**

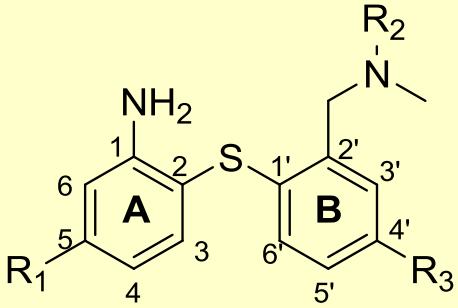

R_1 = CN, R_2 = $^{11}CH_3$, R_3 = H, **[^{11}C]DASB**
R_1 = $^{11}CH_3$, R_2 = CH_3, R_3 = H, **[^{11}C]MADAM**
R_1 = ^{18}F, R_2 = CH_3, R_3 = H, **5-[^{18}F]FADAM**
R_1 = H, R_2 = CH_3, R_3 = $O(CH_2)_3{}^{18}F$, **4'-[^{18}F]FPBM**

1. **SERT selectivity**
2. **^{11}C vs ^{18}F**
3. **Synthetic feasibility**

Drug Design

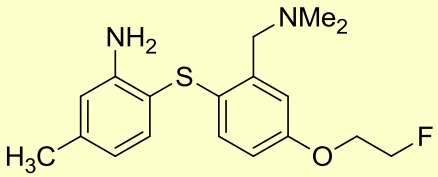

FE-methylADAM

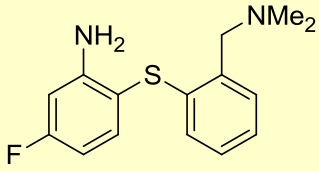

FADAM

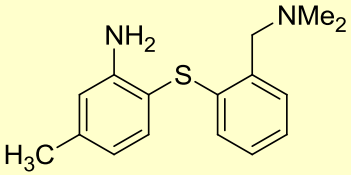

methylADAM

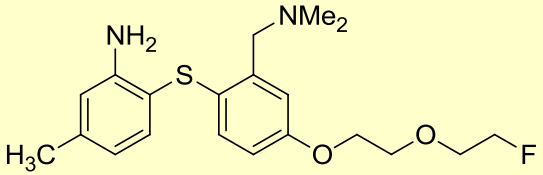

FEE-methylADAM

1. **Synthetic feasibility**
2. **Drug-like properties**

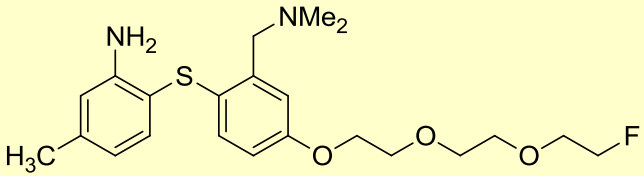

FEEE-methylADAM

Scheme 1

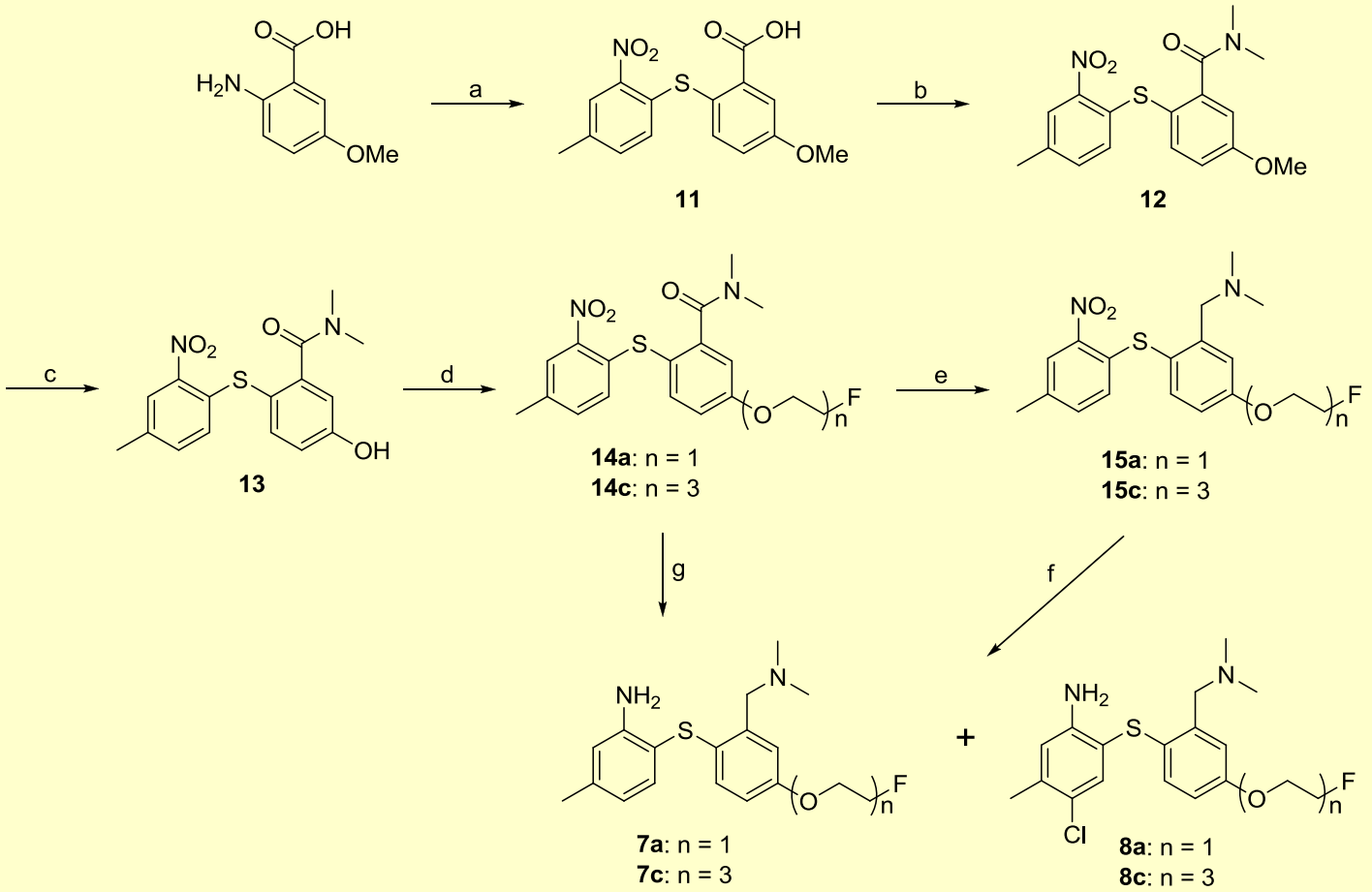

[a] Reagents and conditions: (a) (i) 50% $NaOH_{(aq)}$, $NaNO_2$, H_2O, rt, (ii) $HCl_{(conc.)}$, -10°C, (iii) KS_2COEt, H_2O, 80°C, (iv) 1-bromo-4-methyl-2-nitrobenzene, EtONa, reflux; (b) (i) $(COCl)_2$, DMF, CH_2Cl_2, rt, (ii) Et_3N, Me_2NH, CH_2Cl_2, rt; (c) BBr_3-Me_2S, 1,2-dichloroethane, 70°C; (d) 2-fluoroethyl-4-toluenesulfonate, Cs_2CO_3, DMF, 75°C for **15a** and 1-(2-(2-chloroethoxy)ethoxy)-2-fluoroethane, NaI, Cs_2CO_3, DMF, 75°C for **15c**; (e) (i) BH_3-THF (5 eq), THF, reflux, (ii) $HCl_{(conc.)}$, (iii) H_2O, reflux; (f) $SnCl_2$, $HCl_{(conc.)}$, MeOH, rt; (g) (i) BH_3-THF (10 eq), THF, reflux, (ii) $HCl_{(conc.)}$, (iii) H_2O, reflux.

Bioorg. Chem., **2020**, 97, 103654.

Binding Affinity

compd	R_1	R_2	R_3	K_i (nM)			K_i ratio	
				SERT	NET	DAT	NET/SERT	DAT/SERT
MADAM	CH_3	H	H	0.25	61	532	244	2128
7a	CH_3	H	$O(CH_2)_2F$	**0.25**	98	13%[a]	**392**	-
7b	CH_3	H	$[O(CH_2)_2]_2F$	0.50	60	11%[a]	120	-
7c	CH_3	H	$[O(CH_2)_2]_3F$	1.32	55	11%[a]	41	-
8a	CH_3	Cl	$O(CH_2)_2F$	**0.11**	77	18%[a]	**700**	-
8c	CH_3	Cl	$[O(CH_2)_2]_3F$	**0.21**	54	6%[a]	**257**	-
7d	H	H	$[O(CH_2)_2]_2F$	0.29	**4.1**	23%[a]	**14**	-
7e	H	H	$[O(CH_2)_2]_3F$	0.43	**5.6**	17%[a]	**13**	-
7f	F	H	$[O(CH_2)_2]_2F$	**0.12**	9.2	9%[a]	**77**	-
7g	F	H	$[O(CH_2)_2]_3F$	**0.20**	12	14%[a]	**60**	-

[a] Inhibition percentage under 0.1 μM

Bioorg. Chem., **2020**, 97, 103654.

Lipophilicity and BBB permeability

Compd	Log P_{cal}	Log D_{exp}	P_e
7a	3.83	3.64	81
8a	4.39	4.55	30
7b	3.67	3.53	83
7c	3.52	3.43	73
8c	4.07	4.38	48
7d	3.18	3.37	83
7e	3.03	3.30	91
7f	3.34	3.70	51
7g	3.19	3.63	68
MADAM	3.76	3.87	
Theophylline	—	—	0
Verapamil	—	—	100

Bioorg. Chem., **2020**, 97, 103654.

Metabolic Stability

compd	n	R_1	R_2	Parent compound left after 30 min, (%)[a]	$LogD_{7.4}$
7a	1	Me	H	41	3.64
7b	2	Me	H	60	3.53
7c	3	Me	H	62	3.43
7d	2	H	H	54	3.37
7f	2	F	H	64	3.70
8a	1	Me	Cl	18	4.55
3	-	F	H	0	3.87

Bioorg. Chem., **2020**, 97, 103654.

Scheme 4

Scheme 4[a]

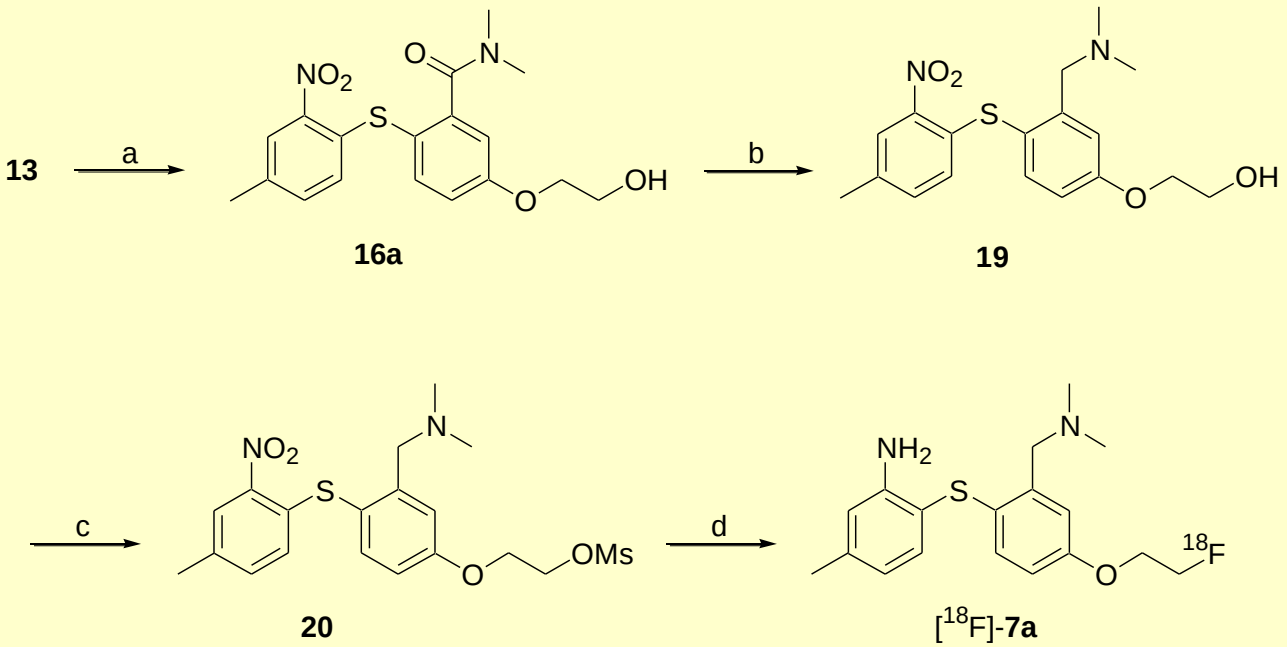

[a] Reagents and conditions: (a) $_2$-bromoethanol, Cs_2CO_3, NaI, DMF, $_{70}{}^{o}C$; (b) (i) BH_3-THF ($_5$ eq), THF, reflux, (ii) $HCl_{(conc.)}$, (iii) H_2O, reflux; (c) MsCl, Et_3N, CH_2Cl_2, rt; (d) (i) K[^{18}F], K_{222}, DMSO, (ii) $NaBH_4$, EtOH, $_{80}{}^{o}C$.

Bioorg. Chem., **2020**, 97, 103654.

Radiosynthesis using Synthesizer

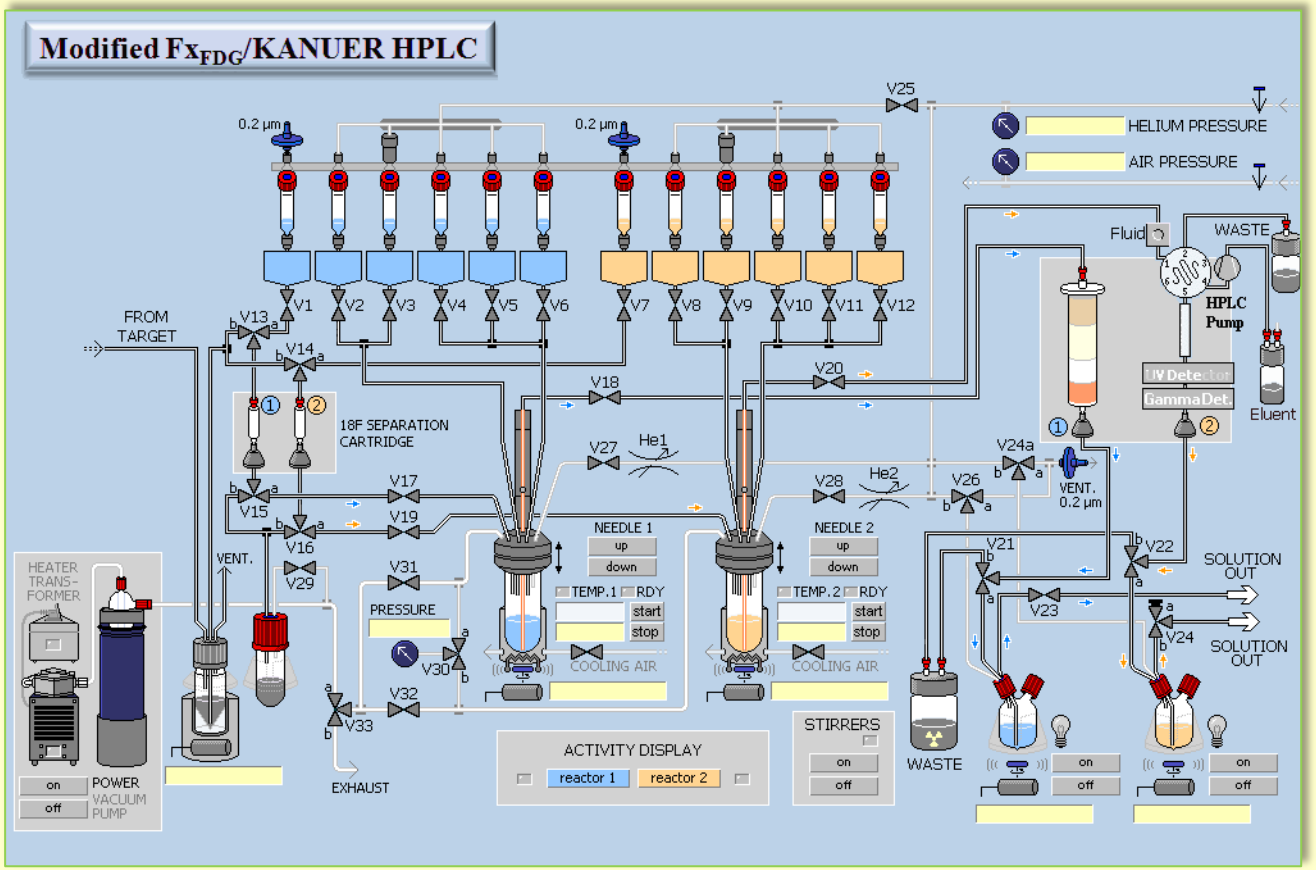

Bioorg. Chem., **2020**, 97, 103654.

PET Imaging in Rat Brain

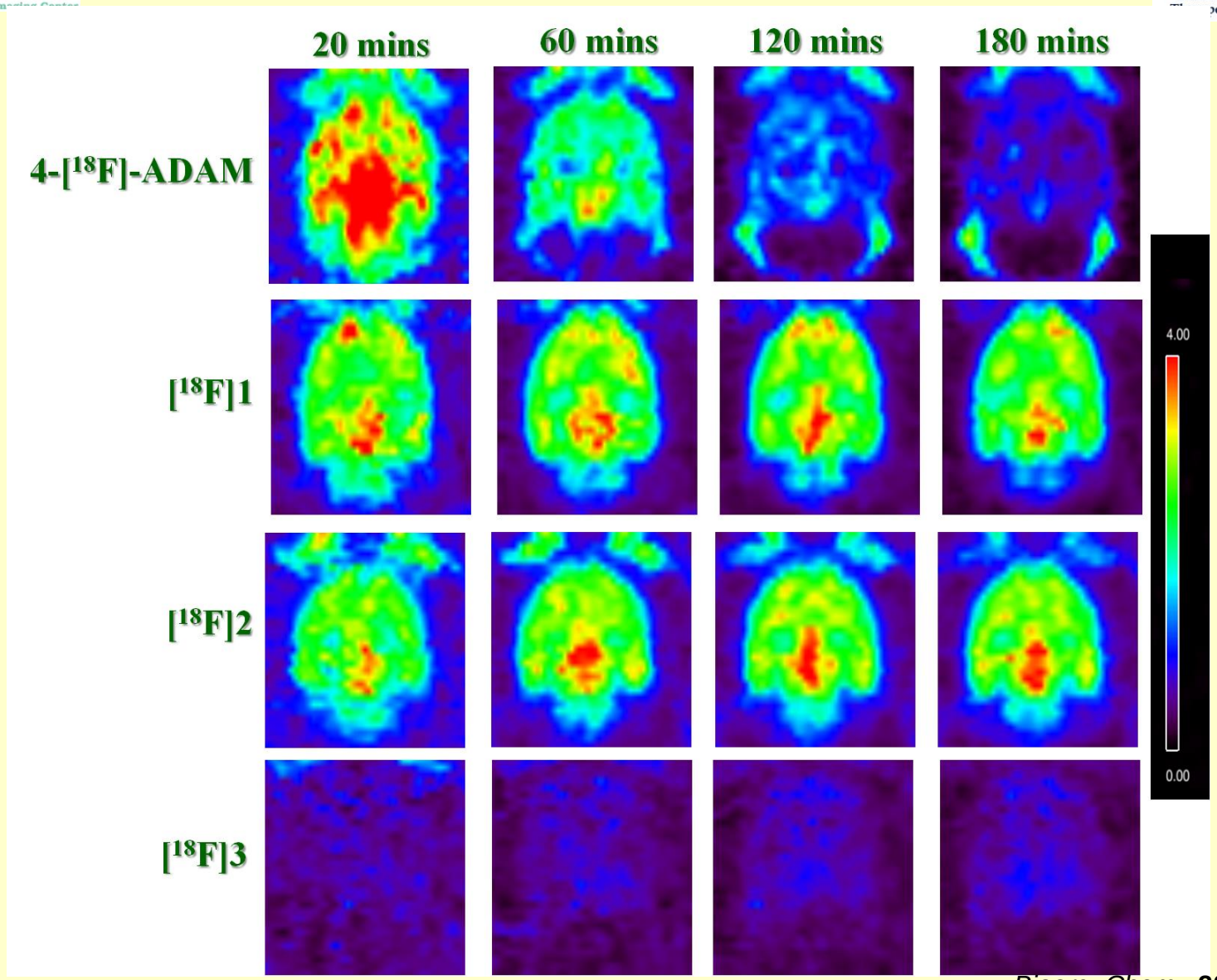

Bioorg. Chem., **2020**, 97, 103654.

Distribution in Rat Brain

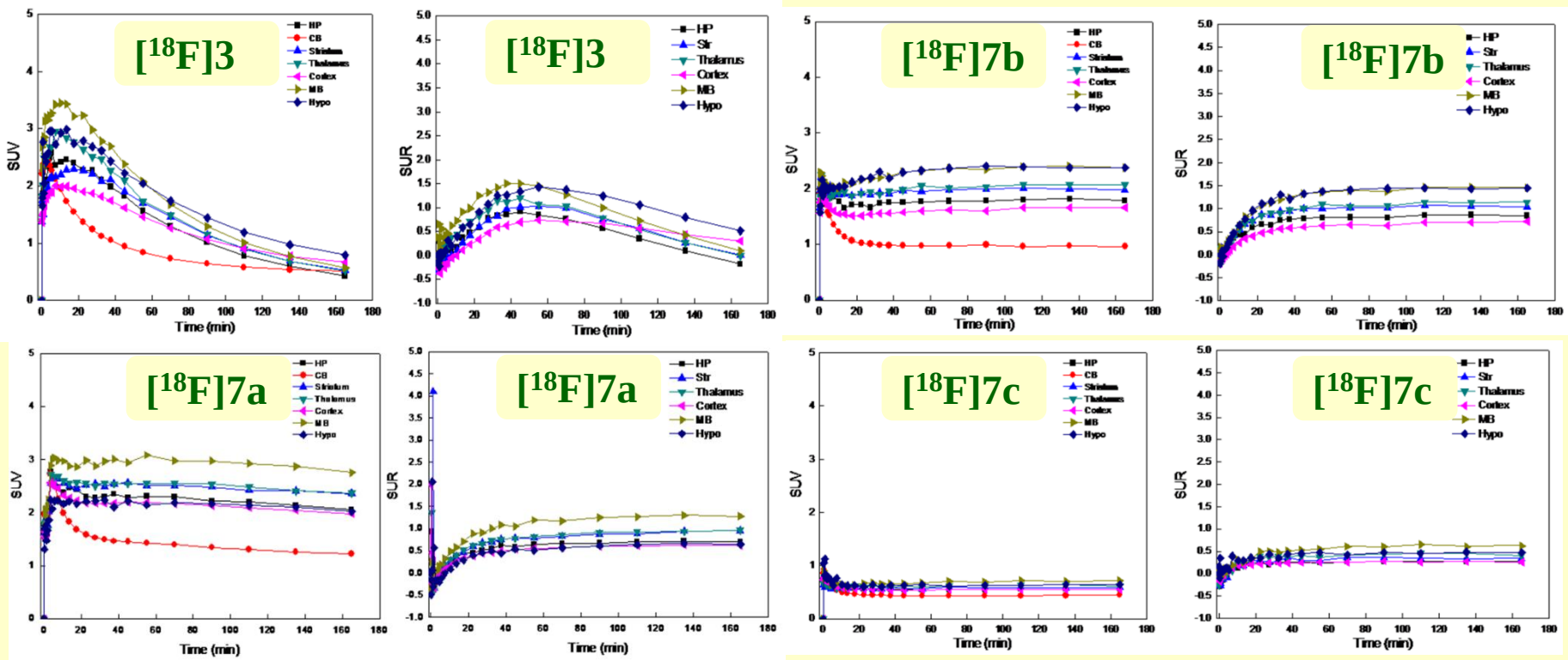

SUV **SUR** **SUV** **SUR**

Bioorg. Chem., **2020**, 97, 103654.

Distribution in Rat Brain

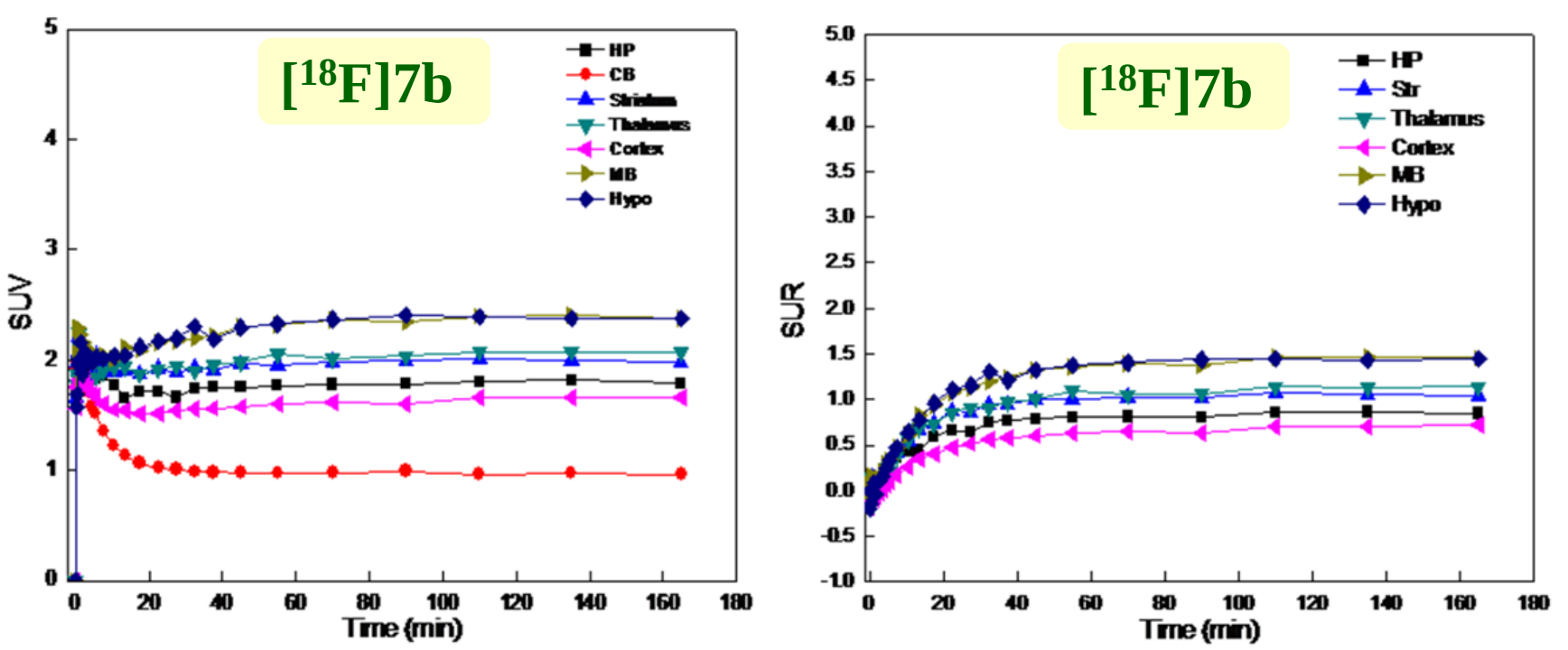

SUV

SUR

Bioorg. Chem., **2020**, 97, 103654.

Summary

- **Two** novel series of fluoropegylated diarylsulfide derivatives were synthesized and possessed **potent** and **selective** SERT binding affinity.
- The target compounds demonstrated **high BBB permeability** in PAMPA assay.
- In PET study, [^{18}F]-**7b** exhibited **significant BBB uptake** and **selective accumulation** in **SERT**–rich regions in the rat brains.

Early *in vivo* Pharmacokinetic Study for Drug Discovery

Dynamic Distribution using PET

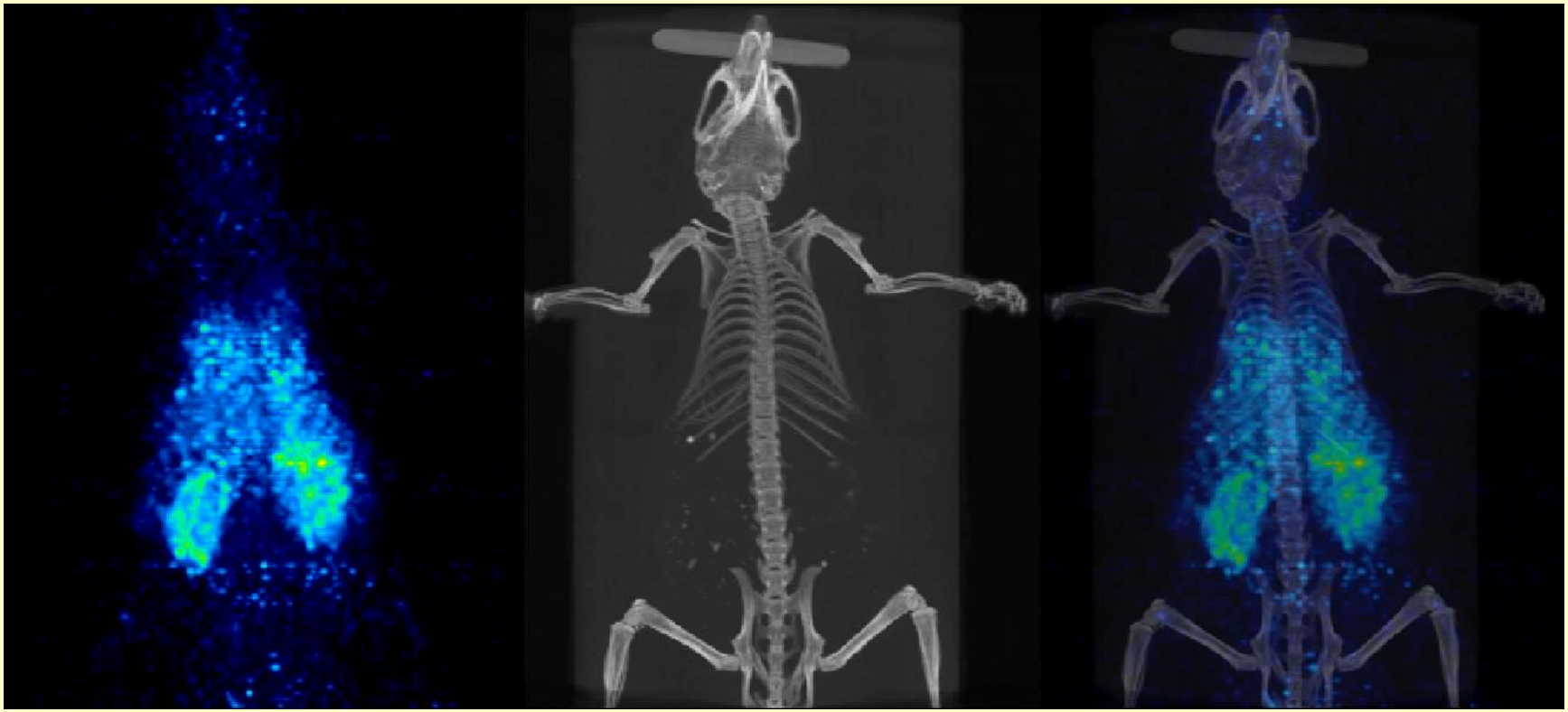

tail vein injection

- 0~60 min
- **300 X**

Dynamic Distribution using PET

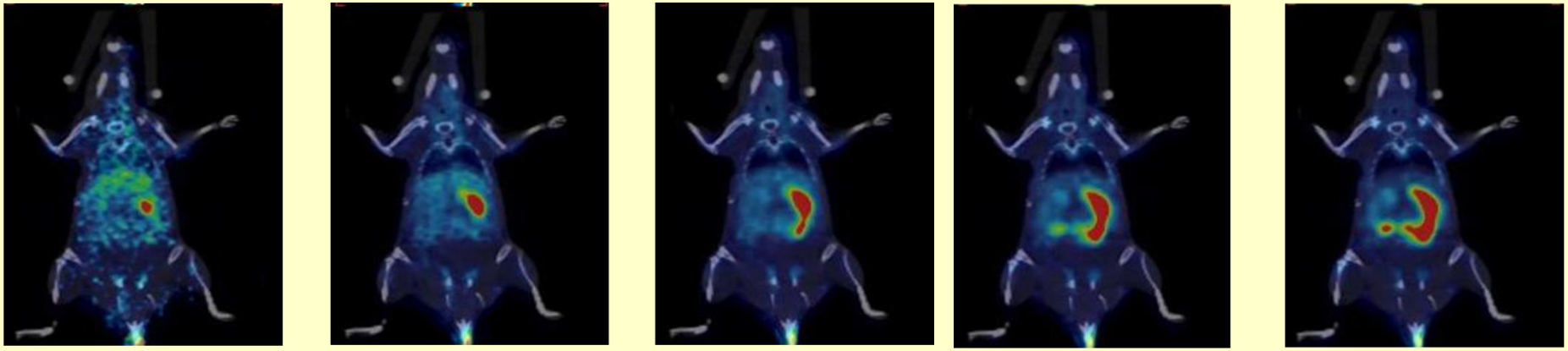

6-8 min | 14-16 min | 22-30 min | 38-46 min | 46-66 min

0~60 minutes after tail vein injection

- Most **accumulated** in **abdominal** organs
- **Peripheral selectivity** may result in less potential toxicity.

NTU SPARK

Acknowledgement

- ***School of Pharmacy , NTU***

  Dr. Li-Te Chang

  Chia-Ying Yang

  Yi-Ying Lin

  Ying-Heng Chen

  Zih-Rou Huang

  Hsin-Yi Shen

- ***Department of Nuclear Medicine, NTUH***

  Prof. Chyng-Yann Shiue

  Prof. Kai-Yuan Tzen

  Prof. Ruoh-Fang Yen

  Dr. Ya-Yao Huang